EXTREMUM SEEKING CONTROL AND ITS APPLICATION TO PROCESS AND REACTION SYSTEMS : A SURVEY

Denis Dochain[1], Michel Perrier[2], Martin Guay[3]
[1]CESAME, Université catholique de Louvain, Louvain-la-Neuve, Belgium
[2]Département de Génie Chimique, École Polytechnique de Montréal, Montréal, Canada
[3]Department of Chemical Engineering, Queen's University, Kingston, Ontario, Canada

Corresponding author: Denis Dochain, Honorary Research Director FNRS, CESAME, Université catholique de Louvain, 4-6 avenue G. Lemaître, 1348 Louvain-la-Neuve, Belgium, denis.dochain@uclouvain.be

Abstract. The objective of this paper is to present a survey on extremum seeking control methods and their applications to process and reaction systems. Two important classes of extremum seeking control approaches are considered : perturbation-based and model-based methods.

Keywords. extremum seeking control, adaptive control.

1 Introduction

Most adaptive control schemes documented in the literature [15]-[17],[20] are developed for regulation to known set-points or tracking known reference trajectories. In some applications, however, the control objective could be to optimize an objective function which can be a function of unknown parameters, or to select the desired states to keep a performance function at its extremum value. Self-optimizing control and extremum seeking control are two methods to handle these kinds of optimization problems. The goal of self-optimizing control is to find a set of controller variables which, when kept at constant set-points, indirectly lead to near-optimal operation with acceptable loss [8][25][29]. The task of extremum seeking is to find the operating set-points that maximize or minimize an objective function. Since the early research work on extremum control in the 1920's [21], many successful applications of extremum control approaches have been reported, for example, fuel flow control to achieve maximum pressure [32], combustion process control for IC engines and gas furnaces [1][28], and anti-lock braking system control [6].

Real-time optimization has seen a resurgence of interest in the recent years. The traditional approach is the model-based repeated optimization where the model is adapted using the available measurements and numerical optimization is performed on the updated model [24][37]. An alternative approach to real-time optimization is known extremum seeking. Extremum seeking control allows the solution of the optimization problem as a *control problem* with the advantages related to sensitivity reduction and disturbance rejection.

In the past few years, Krstic et al. [18][19][33] have presented several schemes for extremum-seeking control of nonlinear systems. First the system is perturbed using an external excitation signal in order to numerically compute the gradient [3][19]. The excitation can also be possibly generated internally by sliding mode control [36]. Their framework allows the use of black-box objective functions with the restriction that the objective value to be minimized is measured on line. Although this technique has been proven useful for some applications [34], the lack of guaranteed transient performance of the black-box schemes remains a significant drawback in its application. Alternatively an adapted model of the system is used for analytical evaluation of the gradient [9]. The extremum seeking framework proposed by Guay and Zhang [9] assumes that the objective function is explicitly known as a function of the system states and uncertain parameters from the system dynamic equations. Parametric uncertainties make the on-line reconstruction of the true cost impossible such that only an estimated value based on parameter estimates is available. The control objective is to simultaneously identify and regulate the system to the lowest cost operating point, which depends on the uncertain parameters. The main advantage of this approach is that one can guarantee some degree of transient performance while achieving the optimization objectives when a reasonable functional approximation of the objective function is available.

The paper is organized as follows. In Section 2 we shall concentrate on the first class of methods, i.e. *perturbation-based extremum-seeking control* methods while Section 3 is dedicated to the second class of methods, i.e. *model-based extremum-seeking control*. In both cases, theoretical results are provided and the performance are illustrated in numerical simulations.

2 Perturbation-based extremum-seeking control

2.1 The basic scheme

The problem addressed is the steady-state optimization of a nonlinear dynamical system stated as follows :

$$\min_{\theta} J(x,\theta) \quad \text{subject to } \dot{x} = F(x,\theta) \equiv 0$$

where $x \in \mathbb{R}^n$ is the state, $\theta \in \mathbb{R}^m$ is the control input, $F : \mathbb{R}^n \times \mathbb{R}^m \to \mathbb{R}^n$ is a smooth function describing the dynamics and $J : \mathbb{R}^n \times \mathbb{R}^m \to \mathbb{R}$ the objective function. The class usually considered in the literature consists of systems that can be represented by a cascade of a static nonlinearity and a linear dynamics. To solve this optimization problem on line, the following extremum-seeking controller is derived from the necessary conditions of optimality under the assumption that the function J is convex :

$$\dot{\theta} = k\frac{dJ}{d\theta} = k\left(\frac{\partial J}{\partial \theta} - \frac{\partial J}{\partial x}\left(\frac{\partial F}{\partial x}\right)^{-1}\frac{\partial F}{\partial \theta}\right) \tag{1}$$

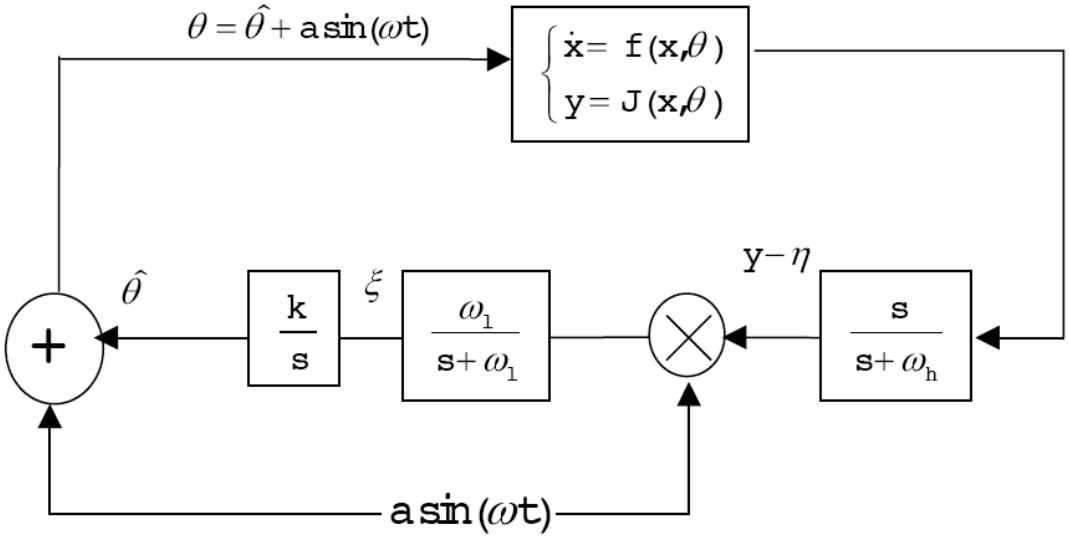

Figure 1: *Extremum seeking control via perturbation method inspired from [19]*

The main challenge of extremum-seeking is the gradient estimation and the perturbation based schemes add an excitation signal to the input in order to extract this information (Figure 1). Note that the objective function is supposed to be directly measured ($y = J(x,\theta)$).

A high pass filter with cutoff frequency ω_h isolates the variations of this optimized variable from its average value. The state that represents the high pass filter is denoted by η. This signal is then modulated by the same excitation signal. A low pass filter with cutoff frequency ω_l and output ξ will filter the resulting signal in order to get the required gradient, $\xi = \frac{dJ}{d\theta}$. Finally an integral controller with gain k drives this estimated gradient to zero.

The scheme can be summarized using the following equations :

$$\dot{\hat{\theta}} = k\xi, \qquad \theta = \hat{\theta} + a\sin(\omega t) \tag{2}$$

$$\dot{\xi} = -\omega_l \xi + \omega_l (y-\eta) a\sin(\omega t) \tag{3}$$

$$\dot{\eta} = -\omega_h \eta + \omega_h y \tag{4}$$

The value of the states at steady-state obtained from $\dot{x} = F(x,\theta) \equiv 0$ is given by $x = l(\theta)$. The cost function at steady-state is given by $y = J(l(\theta),\theta)$. Deviation variables are then considered: $\tilde{\theta} = \hat{\theta} - \theta^*$, $\tilde{y} = y - y^*$ and $\tilde{\eta} = \eta - y^*$ where y^* is the minimum value of the cost function at steady-state y obtained for $\theta = \theta^*$. Then the relationship between $\tilde{y}$ and $\tilde{\theta}$ is expressed as :

$$\tilde{y} = J(l(\theta^* + \tilde{\theta}), \theta^* + \tilde{\theta}) - J(l(\theta^*),\theta^*) \equiv \nu(\tilde{\theta}) \tag{5}$$

If we assume that x is at steady state, the averaged system for the three remaining variables (θ, ξ, and η) is obtained by taking the average of the right hand side over $[0, \frac{2\pi}{\omega}]$. The averaged states are denoted by the superscript $(\cdot)^a$.

The averaged system reads [16] :

$$\frac{d}{dt}\begin{bmatrix}\tilde{\theta}^a\\ \xi^a\\ \tilde{\eta}^a\end{bmatrix}=\begin{bmatrix}k\xi^a\\ -\omega_l\xi^a+\frac{\omega_l\omega}{2\pi}a\int_0^{\frac{2\pi}{\omega}}\nu(\tilde{\theta})\sin(\omega t)dt\\ -\omega_h\tilde{\eta}^a+\frac{\omega_h\omega}{2\pi}\int_0^{\frac{2\pi}{\omega}}\nu(\tilde{\theta})dt\end{bmatrix} \tag{6}$$

where $\tilde{\theta}=\widetilde{\theta}^a+a\sin(\omega t)$. The convergence is shown in [19] by considering the following steps. The exponential stability of the equilibrium point of the above averaged system ($\widetilde{\theta}^a$, ξ^a, and $\widetilde{\eta}^a$) is first proved. Then the exponentially stability of (θ, ξ, and η) (non-averaged) is established using the averaging theorem [16]. Finally this non-averaged system (θ, ξ, and η) acts as the "slow" manifold, while the original system :

$$\dot{x}=F(x,\theta) \tag{7}$$

acts as the boundary layer system which is assumed to be exponentially stable. Then, singular perturbation arguments are considered to show that their interconnection is also exponentially stable [16]. The equilibrium of the averaged system (6) corresponds to :

$$\xi^a=0,\ \int_0^{\frac{2\pi}{\omega}}\nu(\widetilde{\theta})\sin(\omega t)dt=0,\ \tilde{\eta}^a=\frac{\omega}{2\pi}\int_0^{\frac{2\pi}{\omega}}\nu(\widetilde{\theta})dt \tag{8}$$

The value of $\tilde{\theta}^a$ is obtained from the second condition :

$$\int_0^{\frac{2\pi}{\omega}}\nu(\widetilde{\theta^a}+a\sin(\omega t))\sin(\omega t)dt=0 \tag{9}$$

This equation can be analyzed to provide the characteristics of the equilibrium point as summarized in the following result from [19].

Proposition [19] *The equilibrium of the averaged model (6) is a function of the amplitude of the excitation signal :*

$$\tilde{\theta}^a=-\frac{\nu'''(0)}{8\nu''(0)}a^2+O(a^4) \tag{10}$$

2.2 Further analysis of the basic scheme

As already pointed out, perturbation-based extremum-seeking control has been an active research area. We shall concentrate on some specific results that further analyze the performance of this type of extremum-seeking approach. In this section, different results emphasized in [4] are now reported, starting with the dependence of the zero-correlation point on the frequency of the excitation signal.

2.2.1 Dependence of the solution on the perturbation frequency

In the analysis presented in Section 2.1, it was assumed that x and y are at steady state, i.e. the relationship $\tilde{y}=\nu(\tilde{\theta})$ is considered algebraic, yet the relationship is indeed dynamic, $\tilde{y}=P(\tilde{\theta})$, with P being a dynamic operator. The main result is that since the operator is dynamic, it changes the equilibrium point. More specifically the constant value $\widetilde{\theta}^a$ and the sinusoidal excitation $a\sin(\omega t)$ have the same gain, i.e. the gain is independent of the frequency of excitation. This, however, is true only if the system dynamics are neglected. If one accounts for the variation of the gain of the system with the frequency, a dynamic relationship $\tilde{y}=P(\tilde{\theta})$ will be assumed instead of a static relationship $\tilde{y}=\nu(\tilde{\theta})$. The averaged system (6) then becomes :

$$\frac{d}{dt}\begin{bmatrix}\tilde{\theta}^a\\ \xi^a\\ \tilde{\eta}^a\end{bmatrix}=\begin{bmatrix}k\xi^a\\ -\omega_l\xi^a+\frac{\omega_l\omega}{2\pi}a\int_0^{\frac{2\pi}{\omega}}P(\tilde{\theta})\sin(\omega t)dt\\ -\omega_h\tilde{\eta}^a+\frac{\omega_h\omega}{2\pi}\int_0^{\frac{2\pi}{\omega}}P(\tilde{\theta})dt\end{bmatrix} \tag{11}$$

It is shown in [4] that for a general nonlinear system the difference between the optimum and the zero-correlation point is proportional to the square of the frequency.

Theorem 1 *The equilibrium of the averaged model given by (11) is a function of the amplitude and the frequency of the excitation signal :*

$$\tilde{\theta}^a=\alpha a^2+\beta\omega^2+\gamma a^2\omega+\delta\omega^3+O([\omega\ a]^4) \tag{12}$$

where α, β, γ, and δ are constants that could be computed from the Taylor series development of the dynamic operator P. Also, $O([\omega\ a]^4)$ is used to represent $O([\omega\ a]^4)=O(a^4)+O(\omega^4)+O(\omega^2a^2)+O(\omega a^3)+O(a\omega^3)$.

Proof : see [4].

The most important consequence of Theorem 1 is that even if $a \to 0$, the zero-correlation point does not go to the optimum, the error being a function of ω^2:

$$\lim_{a\to 0} \tilde{\theta}^a = \beta\omega^2 + \delta\omega^3 + O(\omega^4) \tag{13}$$

Comparing the current result in [19], the key difference is the presence of terms of the type $O(\omega^2)$. This means that when too high a dither frequency is used, and even if a phase compensation is added such that the evolution is stable, the solution may not necessarily converge to the optimum value. However if the phase compensation is perfect, then the error goes to zero.

2.2.2 Wiener and Hammerstein models

Wiener or Hammerstein models are widely used to represent nonlinear dynamic systems [35]. Such models have linear dynamics and a static nonlinearity. The difference between Wiener and Hammerstein models come from the order in which the linear and nonlinear blocks are placed. The Wiener model consists of a static nonlinearity followed by a linear dynamics while it is the reverse in the Hammerstein model. The interesting aspect of these models is that, at the optimum, the gain of the static part, denoted G_{11}, that multiplies the linear dynamics, is zero for all frequencies. When this fact is used in Theorem 1, it can be seen that the coefficients of ω^2 and ω^3, i.e. β and δ are both equal to zero. It can then be shown that when $G_{11} = 0$ for all frequencies, all terms independent of a in $\tilde{\theta}^a$, i.e. ω^4, ω^5, etc.,. are all zeros.

Theorem 2 *If the nonlinear dynamic system (7) is represented by a Wiener or a Hammerstein model, then the equilibrium of (11) is given by :*

$$\tilde{\theta}^a = \alpha a^2 + \gamma a^2\omega + O(a^2\omega^2) + O(a^4) \tag{14}$$

Proof : see [4].

The consequence of this result is that for a Wiener or a Hammerstein model the distance between the zero-correlation point and the optimum goes to zero as $a \to 0$, i.e. :

$$\lim_{a\to 0} \tilde{\theta}^a = 0 \tag{15}$$

Note that the error is also proportional to $O(a^2)$ due to the absence of terms of the type $O(a\omega)$. However even for a Wiener or Hammerstein representation, for $a \neq 0$, the equilibrium point will indeed be affected by the frequency. Another interesting result can be stated when the static nonlinearity of a Wiener or Hammerstein model is symmetric around the optimum.

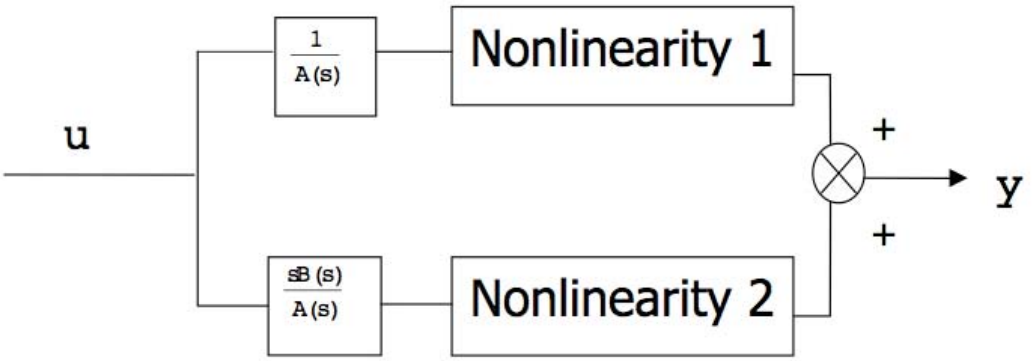

Figure 2: *Approximation of a general nonlinear system using two parallel Hammerstein models*

Lemma 1 *Let the system (7) be represented by a Wiener or a Hammerstein model wherein the static nonlinearity is an even function of $\tilde{\theta}$. Then $\tilde{\theta}^a = 0$ is an the equilibrium of (11).*

Proof: see [4].

This result states that the error comes from the asymmetry of the static nonlinearity. Note however that nothing much can be said if the nonlinearity cannot be represented by a Wiener or Hammerstein model. This means that from an optimization perspective, certain nonlinear systems behave differently from their Wiener/ Hammerstein approximations. At the steady-state optimum, the gain is zero for all frequencies with Wiener or Hammerstein approximation. However at the steady-state optimum of a nonlinear dynamic system, though the static gain is zero, the gain at other frequencies is typically non-zero. This aspect can be captured by representing a nonlinear dynamic system as a sum of two Wiener or Hammerstein models (Figure 2). The first branch has a zero gain at the static optimum while the second has nonzero gain.

2.2.3 Illustrative Example

An isothermal reaction system in a plug flow reactor with distributed feed [5] and the following reaction scheme $A \rightarrow B \rightarrow C$, $2A \rightarrow D$ is considered to illustrate the dependence of the zero-correlation point with frequency. Its dynamics are given by the following set of PDE's :

$$\frac{\partial C_A}{\partial t} = -\frac{v}{S}\frac{\partial C_A}{\partial z} - \frac{C_A}{S}\frac{\partial v}{\partial z} + \frac{q}{S}C_{Ain}^{dist} - k_1 C_A - 2k_3 C_A^2 \quad (16)$$

$$\frac{\partial C_B}{\partial t} = -\frac{v}{S}\frac{\partial C_B}{\partial z} - \frac{C_B}{S}\frac{\partial v}{\partial z} + k_1 C_A - k_2 C_B \quad (17)$$

$$\frac{\partial v}{\partial z} = q \quad (18)$$

$$C_A(z,0) = C_{A0}, C_B(z,0) = C_{B0},\ C_A(0,t) = C_{Ain}, C_B(0,t) = C_{Bin} \quad (19)$$

with C_X, q, k_i, C_{Ain}, C_{Ain}^{dist}, S, L the concentration of species X, the volumetric flowrate per unit length, the rate constants, the inlet concentration, the distributed feed concentration; the volumetric flowrate, the reactor section, and the reactor length, respectively. The objective is to maximize the concentration of product B at the reactor output, $C_B(L)$, and the manipulated variable is q. The parameter values are equal to :

$$\begin{aligned} k_1 &= 5.6530\,\mathrm{h}^{-1}, k_2 = 5.6530\,\mathrm{h}^{-1}, k_3 = 140.26011\,\mathrm{mol}^{-1}\,\mathrm{h}^{-1} \\ C_{Ain} &= 1\,\mathrm{mol\,l}^{-1}, C_{Ain}^{dist} = 10\,\mathrm{mol\,l}^{-1}, v = 1\,\mathrm{m}^3\,\mathrm{h}^{-1}, L = 1\,\mathrm{m} \end{aligned} \quad (20)$$

Table 2.1: Influence excitation frequency on the equilibrium value

Excitation frequency$[h^{-1}]$	k_{opt}	τ_h $[h]$	τ_l $[h]$	Equilibrium $[h^{-1}]$
0.0100	0.0100	1000	1000	2.1024
0.0464	0.0464	215.50	215.50	2.0911
0.1292	0.1292	77.40	77.40	2.0821
0.5995	0.5995	16.70	16.70	1.8712
1.0000	1.0000	10.00	10.00	1.5115

The system under study is linearized at three operating points, $q = q_{opt}$, $q_{opt} + 0.5$, $q_{opt} - 0.5$. The pole-zero maps of the three operating points tell us most of the poles are zeros do not change the position except one zero near the origin. The system shifts from minimum phase to non-minimum phase while it behaves as a filtered differentiator at the optimum. So this system cannot be represented by Wiener or Hammerstein models and has to be approximated locally by two parallel branches (Figure 2).

As summarized in Table 2.1 and Figure 3, several excitation signal frequencies are used and the converged zero-correlation points obtained by simulation of the nonlinear model given by (16)-(19) are compared to the static optimum dilution rate 2.1006 h^{-1}. Note that initial conditions are chosen to be in the local stability region [19]. If the initial conditions are chosen in this region, the equilibrium point is independent of the initial condition. It is interesting to note that the error is small until a certain cutoff frequency, and increases drastically when the frequency is larger than this value.

3 Model-based extremum-seeking control

3.1 General problem, basic model and assumptions

An alternative to the perturbation-based extremum seeking control consists of considering explicitly a dynamical model of the system with unknown parameters, and to combine optimum search and adaptive control to guarantee converge of the closed-loop system to the optimum operating points. Such an approach has been largely developed in a number of papers dedicated to the real-time optimization of bioprocesses [10][22][23][30][31][38], chemical reactors [5][11][13][14], pulp and paper processes [7] and biomedical systems [12]. In order to keep the presentation as simple as possible, we shall consider in the present paper a simple example of a bioreactor with two different options. In the first instance, the kinetics model structure is assumed to be known while its parameters are unknown [38]. In the second instance, the kinetics model is assumed to be unknown and an universal approximation is considered to update the model kinetics and drive the system to its optimum [10].

Consider the following microbial growth model :

$$\dot{x} = \mu(x,s)x - ux \quad (21)$$

$$\dot{s} = -k_1\mu(x,s)x + u(s_0 - s) \quad (22)$$

$$y = k_2\mu(x,s)x \quad (23)$$

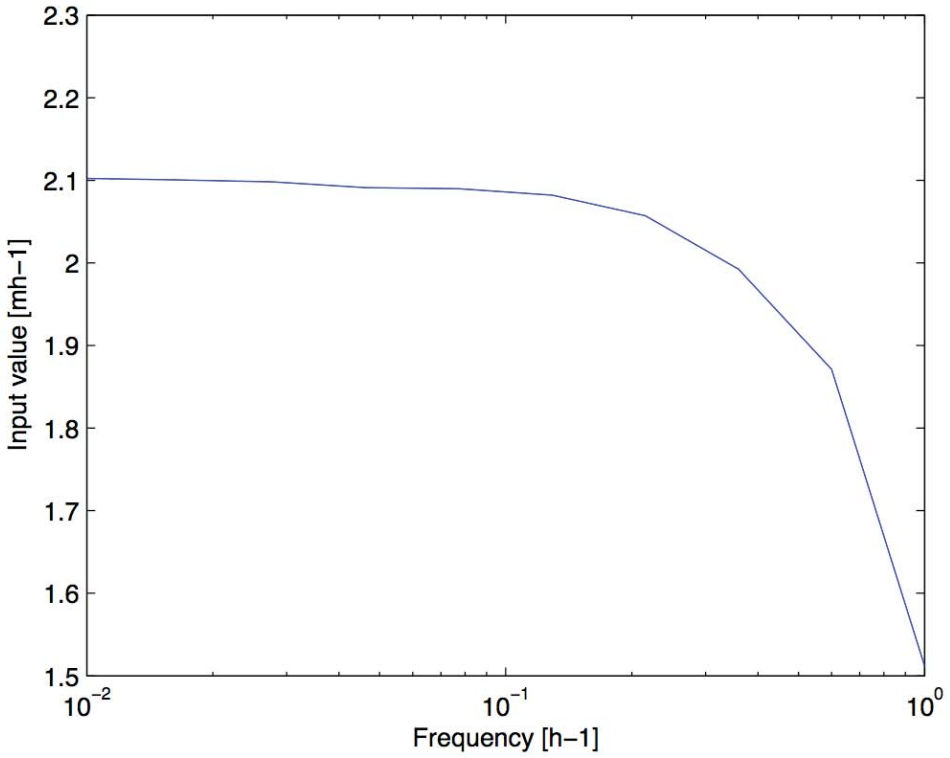

Figure 3: *Evolution of the solution as a function of the excitation signal frequency*

where states $x \in [0,+\infty)$ and $s \in [0,+\infty)$ denote biomass and substrate concentrations, respectively, $u \geq 0$ is the dilution rate, y is the production rate of the reaction product, s_0 denotes the concentration of the substrate in the feed, and $k_1, k_2 > 0$ are yield coefficients.

The nonlinear function $\mu(s)$ denotes the growth rate of the process. System (21)(22) can represent a large class of biochemical processes depending on the choice of the growth rate $\mu(x,s)$. There are many different models for $\mu(x,s)$ proposed in the literature [2], for example:

$$\mu(x,s) = \mu(s) = \frac{\mu_m s}{K_s + s} \quad \text{(Monod)} \tag{24}$$

$$\mu(x,s) = \frac{\mu_m s}{K_c x + s} \quad \text{(Contois)} \tag{25}$$

$$\mu(x,s) = \frac{\mu_m K_0 s}{1 + K_1 s + K_2 s^2} \quad \text{(Haldane)} \tag{26}$$

where $\mu_m > 0$ is the maximum value of the specific growth rate, and positive constant K_s, K_c and K_0 to K_2 denote the coefficients for different growth rate models.

3.2 Case #1 : the specific growth rate model structure is known

Let us first consider that the specific growth rate model structure μ is known and follows (for instance) Monod kinetics (24). Let us also considerthat only s and y are measurable, and that the biomass concentration x is not available for measurement. However the scheme developed in this paper is not limited to this model and can be easily extended to the plants with other growth rate representations. The control objective is to design a controller u such that the production rate y achieves its maximum.

We first calculate the system's equilibria corresponding to a constant dilution rate u_e. By setting the right-hand side of (21)(22) to zero, we obtain two equilibria. The first is $x_e = 0$ and $s_e = s_0$ which is called the wash-out equilibrium. The second is :

$$s_e = \frac{K_s u_e}{\mu_m - u_e}, \quad x_e = \frac{s_0 - s_e}{k_1}$$

At the steady-state, the production rate can be expressed by :

$$y_e(s_e) = \frac{k_2 \mu_m s_e (s_0 - s_e)}{k_1 (K_s + s_e)} \tag{27}$$

From (22) and (24), we have :

$$\frac{\partial y_e(s_e)}{\partial s_e} = \frac{-k_2\mu_m}{k_1(K_s+s_e)^2}\left(s_e^2+2K_ss_e-s_0K_s\right) \tag{28}$$

$$\frac{\partial^2 y_e(s_e)}{\partial s_e^2} = \frac{-2k_2\mu_m}{k_1(K_s+s_e)^3}\left(K_s^2+s_0K_s\right) \tag{29}$$

It is shown that $\frac{\partial^2 y_e(s_e)}{\partial s_e^2} > 0, \forall s_e \geq 0$. Hence at the equilibrium, $y_e(s)$ has a maximum :

$$y^* = y_e(s^*) = \frac{k_2\mu_m s^* x^*}{K_s+s^*} \tag{30}$$

with :

$$s^* = \sqrt{K_s^2+s_0K_s}-K_s,\ x^* = \frac{s_0-s^*}{k_1}. \tag{31}$$

From the above analysis, we know that if the substrate concentration s can be stabilized at the set-point s^* then the production rate y is maximized. However, since the exact values of the Monod's model parameters K_s and μ_m are usually unknown, the desired set-point s^* is not available. An adaptive extremum seeking algorithm is now presented to search this unknown set-point such that the production rate y is optimized.

Assumption 1 *The upper bound of K_s is known, i.e. $K_s \leq K_{s0}$ with known constant $K_{s0} > 0$.*

Let us define $\theta = [\theta_s\ \theta_\mu\ \theta_k]^T$ with :

$$\theta_\mu = \frac{\mu_m}{K_s},\quad \theta_s = \frac{1}{K_s},\quad \theta_k = \frac{k_1}{k_2} \tag{32}$$

The mass balance equation for s (22) and the dynamical equation of y that can be deduced from the basic model (21)-(23) can be written as follows :

$$\dot{s} = -\theta_k y + u(s_0-s) \tag{33}$$

$$\dot{y} = -uy + \frac{\theta_\mu s^2 y - \theta_k y^2 + (s_0-s)uy}{s(1+\theta_s s)} \tag{34}$$

Let $\hat{\theta}$, $\hat{s}$ and $\hat{y}$ denote the estimates of θ, s and y, respectively, and consider the following observer-based estimation scheme :

$$\dot{\hat{s}} = -\hat{\theta}_k y + u(s_0-s) + k_s e_s \tag{35}$$

$$\dot{\hat{y}} = -uy + \frac{\hat{\theta}_\mu s^2 y - \hat{\theta}_k y^2 + (s_0-s)uy}{s(1+\hat{\theta}_s s)} + k_y e_y \tag{36}$$

$$\dot{\hat{\theta}}_s = \begin{cases} \dfrac{\gamma_s \phi_s y e_y}{1+\hat{\theta}_s s}, & \text{if } \hat{\theta}_s > 1/K_{s0} \\ & \text{or } \hat{\theta}_s = 1/K_{s0} \text{ and } \phi_s y e_y \geq 0 \\ 0, & \text{otherwise} \end{cases} \tag{37}$$

$$\dot{\hat{\theta}}_\mu = \gamma_\mu s y e_y \tag{38}$$

$$\dot{\hat{\theta}}_k = -\gamma_k y\left(\frac{y}{s}e_y + z_s + e_s\right) \tag{39}$$

with $k_s, k_y, \gamma_\mu, \gamma_s, \gamma_k > 0$, the prediction errors $e_s = s-\hat{s}$ and $e_y = y-\hat{y}$, and the initial condition $\hat{\theta}_s(0) \geq 1/K_{s0} > 0$.

Let us then define the variable z_s :

$$z_s = s - \frac{1}{\hat{\theta}_s}\left(\sqrt{1+s_0\hat{\theta}_s}-1\right) + d(t) \tag{40}$$

where $d(t) \in C^1$ is an excitation signal to be assigned. Let us now consider the following extremum seeking controller :

$$u = -\frac{\gamma_s \beta_a(y,s,\hat{\theta}_s)e_y + \dot{d}(t) - \hat{\theta}_k y + k_z z_s}{[1+\gamma_s\beta_b(y,s,\hat{\theta}_s)e_y](s_0-s)},\ k_z > 0 \tag{41}$$

with :

$$\beta_a(y,s,\hat{\theta}_s) = \begin{cases} \frac{(-\hat{\theta}_\mu s^2+\hat{\theta}_k y)y}{1+\hat{\theta}_s s}\beta(\hat{\theta}_s), & \text{if } \hat{\theta}_s > 1/K_{s0} \\ & \text{or } \hat{\theta}_s = 1/K_{s0} \text{ and } \phi_s y e_y \geq 0 \\ 0, & \text{otherwise} \end{cases} \tag{42}$$

$$\beta_b(y,s,\hat{\theta}_s) = \begin{cases} -\frac{y}{1+\hat{\theta}_s s}\beta(\hat{\theta}_s), & \text{if } \hat{\theta}_s > 1/K_{s0} \\ & \text{or } \hat{\theta}_s = 1/K_{s0} \text{ and } \phi_s y e_y \geq 0 \\ 0, & \text{otherwise} \end{cases} \tag{43}$$

Let us further assume that the gain function k_y is equal to :

$$k_y = k_{y0} + \frac{(s_0 - s)K_{s0}|u|}{2(1+K_{s0}s)},\ k_{y0} > 0 \tag{44}$$

and that in order to avoid the singularity that may happen to the controller (41) when $1+\gamma_s\beta_b(y,s,\hat{\theta}_s)e_y$ approaches zero, a small learning gain γ_s should be used such that :

$$1+\gamma_s\beta_b(y,s,\hat{\theta}_s)e_y > 0 \tag{45}$$

Let us also assume that the dither signal $d(t)$ is designed such that the following condition holds :

$$\lim_{t\to\infty}\frac{1}{T_0}\int_t^{t+T_0}\Phi_a(s,y,\hat{\theta})\Phi_a^T(s,y,\hat{\theta})y^2 d\tau \geq c_0 I,\ c_0 > 0 \tag{46}$$

Theorem 3 *For the system (21)-(23) if the learning rate γ_s is chosen small enough such that (45) holds, and if the dither signal $d(t)$ satisfies the PE condition (46), then the extremum seeking controller (41) with adaptive laws (35)-(39) guarantees that the production rate y converges to an adjustable neighborhood of its maximum y^* :*

$$\lim_{t\to\infty} y = y^* + k_2\mu(s^*)\varepsilon(d,\dot{d}) - \lim_{t\to\infty}\left[k_2 d(t)\int_0^1 \frac{\partial\mu(s_\lambda)}{\partial s_\lambda}d\lambda\right] \tag{47}$$

with :

$$\varepsilon(d,\dot{d}) = \frac{d(t)}{k_1} + \frac{\dot{d}(t)}{k_1\mu(s)} \tag{48}$$

Proof: see [38]. The proof is based on the following Lyapunov function :

$$V = \frac{z_s^2}{2} + \frac{1}{2}\left(\frac{\tilde{\theta}_\mu^2}{\gamma_\mu} + \frac{\tilde{\theta}_s^2}{\gamma_s} + \frac{\tilde{\theta}_k^2}{\gamma_k}\right) + \frac{e_s^2}{2} + (1+\theta_s s)\frac{e_y^2}{2} \tag{49}$$

and considers LaSalle-Yoshizawa's Theorem, LaSalle Invariance Principle and Barbalat's Lemma (see e.g. [15][17]).

To show the effectiveness of the proposed design, simulations have been performed using the experimental conditions provided in [34] with the following parameters and initial states :

$$K_s = 0.2,\ \mu_m = 1.0,\ Y = 0.5,\ k_1 = 2.0,\ k_2 = 1.0,\ s_0 = 10.0,\ x(0) = 3.0,\ s(0) = 0.9$$

The upper bound of K_s is assumed to be known : $K_{s0} = 0.5$. The design parameters are set to :

$$\gamma_s = 2.0,\ \gamma_\mu = 20.0,\ \gamma_k = 2.0,\ \hat{\theta}_s(0) = 8.0,\ \hat{\theta}_\mu(0) = 2.0,\ \hat{\theta}_k(0) = 4.0$$

The dither signal is chosen as $d(t) = 2.2 - \cos(0.5t) - \cos(0.3t)$. It is shown from Figure 4 that the production rate reaches its maximum value 3.77 after $t = 6$. Due to the injection of the excitation signal $d(t)$, the production rate keeps oscillating around the optimal point. Figure 5 plots the control input. The convergence of the algorithm can be confirmed by inspection of a simulation performed over a longer time period (*i.e.* $t = 800$). In order to remove the effect of the excitation signal $d(t)$, we let $d(t)$ vanish exponentially as $t > 600$. The production rate is shown in Figure 6. The simulation confirm that the production rate converges to its maximum

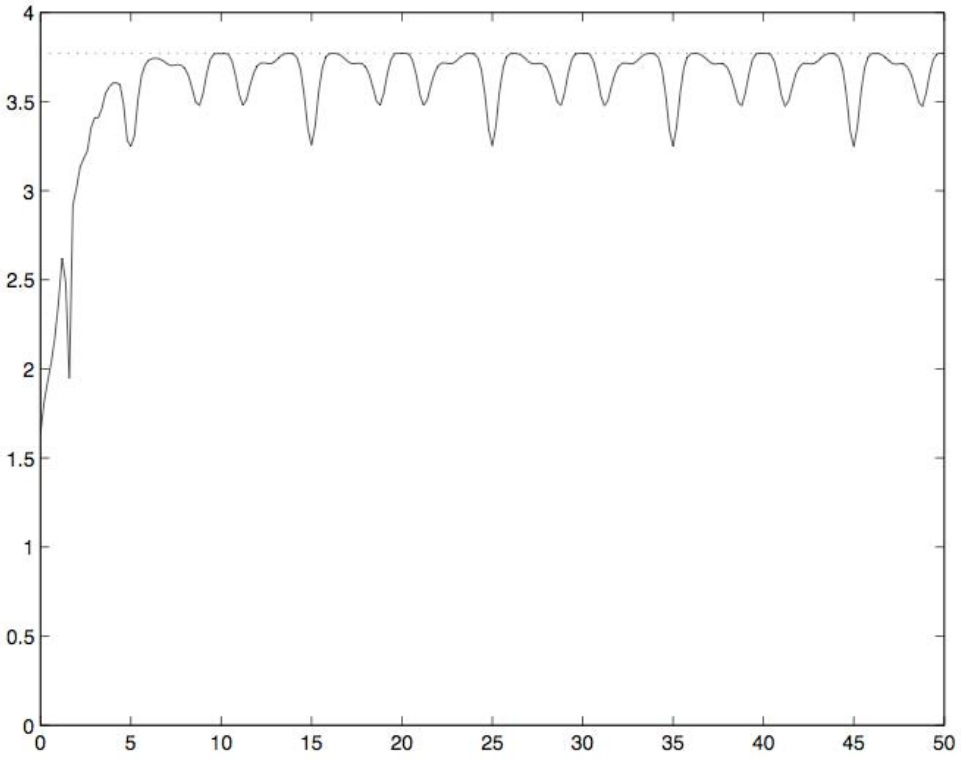

Figure 4: *Production rate y ("—") and its maximum y* ("- -")*

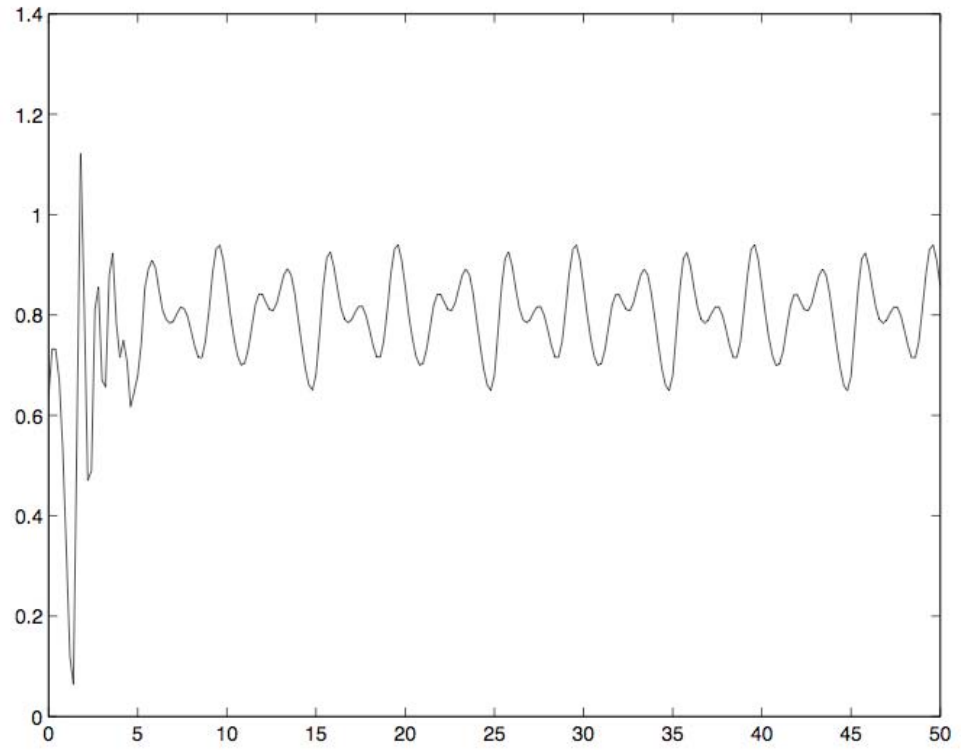

Figure 5: *Control input $u(t)$*

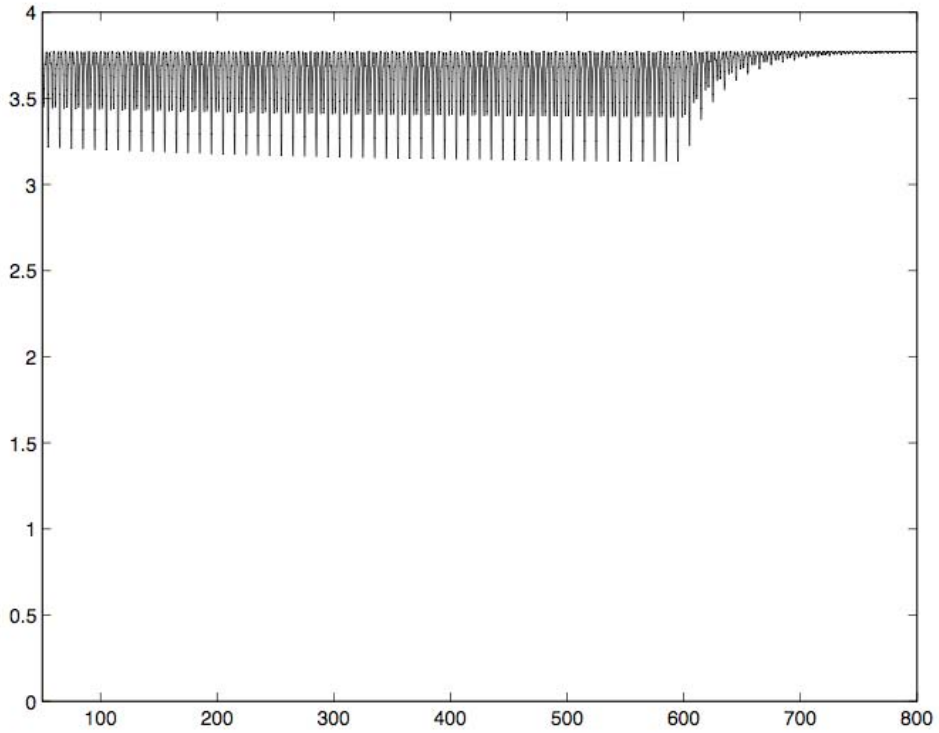

Figure 6: *Production rate y ("—") and its maximum y* ("- -")*

3.2.1 Case#2 : the specific growth rate model structure is unknown

Let us consider the case when the structure of the specific growth rate $\mu(s,x)$ is unknown. In the present instance, in order to emphasize the flexibility of the approach, we consider that s and x are measurable while y is not. Let us choose to parameterize the unknown function $\mu(s)$ via some universal approximation (e.g. a neural network) as :

$$\mu(s(t)) = W^{*^T} S(s(t)) + \mu_l(t) \tag{50}$$

with $\mu_l(t)$ the approximation and $S(s(t))$ the basis function vector :

$$S(s) = [s_1(s), s_2(s), ..., s_l(s)]^T,\ s_i(s) = \exp\left[\frac{-(s-\varphi_i)^T(s-\varphi_i)}{\sigma_i^2}\right],\ i = 1,2,...,l \tag{51}$$

The parameters of the basis function approximation (50) are assumed to take values in a known compact set Ω_w. The functional approximation of the equilibrium manifold is dependent on the center of the receptive field, φ_i, and the width of the Gaussian function σ_i. Universal approximation results stated in [26][27] indicate that if l is chosen sufficiently large, then $W^{*^T} S(s)$ can approximate any continuous function to any desired accuracy on a compact set. For the Neural Network approximation, we assume that the following holds.

Assumption 2 *The Neural Network approximation errors satisfies* $|\mu_l(t)| \leq \bar{\mu}_l$ *with constant* $\bar{\mu}_l > 0$ *over a compact set.*

In this case, Assumption 1 makes sense. The physical nature of the problem is such that the growth rate $\mu(s)$ is inherently bounded. Since the approximation $W^{*^T} S(s)$ is bounded by construction, an upper bound on approximation error can be obtained easily. In the remainder, we will assume that this upper bound is known.

Following (50), the steady-state production rate is approximated by :

$$y_e = \frac{k_2}{k_1} W^{*T} S(s_e)(s_0 - s_e) \tag{52}$$

From (52) we have :

$$\frac{\partial y_e}{\partial s_e} = \frac{k_2}{k_1} W^{*T} \Big(dS(s_e)(s_0 - s_e) - S(s_e) \Big) \tag{53}$$

and

$$\frac{\partial^2 y_e}{\partial s_e^2} = \frac{k_2}{k_1} W^{*T} \Big(d^2 S(s_e)(s_0 - s_e) - 2dS(s_e) \Big) \tag{54}$$

Assuming that the parameter vector W^* is such that $\frac{\partial^2 y_e}{\partial s_e^2} > 0, \forall s_e \geq 0$, then $y_e(s)$ has a maximum at the system equilibrium :

$$y^* = y_e(s^*) = \frac{k_2}{k_1} W^{*T} S(s^*) x^* \tag{55}$$

with :

$$x^* = \frac{s_0 - s^*}{k_1} \tag{56}$$

The objective is to develop a controller that maximizes the steady-state value of the production rate y^*. However, since the exact values of the ideal weights, W^*, are not known *a priori*, they have to be estimated. The estimation scheme is based on the mass balance equations (21)(22) that can be re-expressed as follows :

$$\dot{x} = (W^{*T} S(s) + \mu_l(t))x - ux \tag{57}$$

$$\dot{s} = -k_1 (W^{*T} S(s) + \mu_l(t))x + u(s_0 - s) \tag{58}$$

Let $\hat{W}$ denote the estimate of the true parameter W^* ($\tilde{W} = W^* - \hat{W}$) and let $\hat{s}$ and $\hat{x}$ be the predictions of s and y. The estimation scheme is written as follows :

$$\dot{\hat{x}} = \hat{W}^T S x - ux + k_x e_x + c_1(t)^T \dot{\hat{W}} \tag{59}$$

$$\dot{\hat{s}} = -k_1 \hat{W}^T S x + u(s_0 - s) + k_s e_s + c_2(t)^T \dot{\hat{W}} \tag{60}$$

$$\dot{c}_1^T = -k_x c_1^T + x S^T \tag{61}$$

$$\dot{c}_1^T = -k_s c_2^T - k_1 x S^T \tag{62}$$

$$\dot{c}_3^T = -k_z c_3^T - k_1 x \hat{W}^T \Gamma_2 S^T \tag{63}$$

$$\dot{\hat{W}} = -\gamma_w \Upsilon(t)^T \Upsilon(t) \tilde{W} - \gamma_w \Upsilon(t)^T \eta + \begin{cases} 0 \begin{cases} \text{if } q(\hat{W}) \leq w_m \text{ or} \\ \text{if } q(\hat{W}) \geq w_m \text{ and } \gamma \hat{W}^T \Upsilon(t)^T e \leq 0 \end{cases} \\ \gamma_w \gamma^2 q(\hat{W}) \frac{\hat{W}\hat{W}^T}{\hat{W}^T \hat{W}} \left(\Upsilon(t)^T \Upsilon(t) \tilde{W} + \Upsilon(t)^T \eta \right) \text{ otherwise} \end{cases} \tag{64}$$

with the prediction errors $e_s = s - \hat{s}$ and $e_x = x - \hat{x}$, $\eta^T = [\eta_1, \eta_2, \eta_3]$:

$$\eta_1 = e_x - c_1(t)^T \tilde{W},\ \eta_2 = e_s - c_2(t)^T \tilde{W},\ \eta_3 = z_s - c_3(t)^T \tilde{W} \tag{65}$$

the gain functions $k_s, k_y, k_z > 0$:

$$k_x = k_{x0} + \frac{k_4}{2} x^2,\ k_s = k_{s0} + \frac{k_3 k_5}{2} x^2,\ k_z = k_{z0} + \frac{k_3 k_6}{2} x^2 (\hat{W}^T \Gamma_2)^2 \tag{66}$$

where k_{x0}, k_{s0}, k_{z0}, k_4, k_5 and k_6 are positive constants. The matrix $\Upsilon(t)$ and the function $q(\hat{W})$ are equal to :

$$\Upsilon(t)^T = [c_1(t)\, c_2(t)\, c_3(t)],\ \ q(\hat{W}) = (M(\hat{W}) - w_m^2)/\varepsilon^2 + w_m \varepsilon \tag{67}$$

where $w_m > 0$ and $\varepsilon > 0$ are positive constants.

Since the parameter vector W^* is unknown, the controller is designed to make the system state variables track points where the estimated gradient :

$$z = \frac{k_2}{k_1} \hat{W}^T \Big(dS(s)(s_0 - s) - S(s) \Big) \tag{68}$$

vanishes. In order to ensure that the estimated gradient approaches the true gradient asymptotically, we have to ensure that the parameter estimates approach the optimal weight vector W^*. To achieve this objective, an excitation signal is designed and injected into the adaptive system to ensure convergence of the estimated parameters to their true value.

Let us define :

$$z_s = \hat{W}^T \Big(dS(s)(s_0 - s) - S(s) \Big) - d(t) \tag{69}$$

where $\frac{k_2}{k_1} > 0$ has been removed for simplicity and $d(t) \in C^1$ is a dither signal that follows the following dynamics :

$$\dot{d}(t) = c_3(t)^T \dot{\hat{W}} + \Gamma_1^T \dot{\hat{W}} - k_d d(t) + \hat{W}^T \Gamma_2 a(t) \tag{70}$$

where $a(t)$ is an external signal providing excitation to the process and $k_d > 0$ is a positive gain function to be assigned.

The adaptive extremum seeking controller is then given by the following expression :

$$u = \frac{\left(k_1 \hat{W}^T Sx + a(t) - \frac{k_d}{\hat{W}^T \Gamma_2} d(t) - \frac{k_z}{\hat{W}^T \Gamma_2} z_s\right)}{(s_0 - s)} \tag{71}$$

Theorem 4 *For the system (21)(23) with the observer-based estimator (59)-(63), the controller (71), the dither signal (70) and the adaptive learning law (64), if that the signal $a(t)$ is such that :*

$$\int_t^{t+T} \Upsilon(\tau)^T \Upsilon(\tau) d\tau \geq k_N I_N \tag{72}$$

for positive constants $T > 0$ and $k_N > 0$, then
1) the error dynamics converge exponentially to a small neighborhood of the origin;
2) the parameter estimation errors $\tilde{W}$ converge exponentially to a small neighborhood of the origin;
3) the tracking error from the unknown steady-state z_s converges exponentially to a small neighborhood of the origin.

Proof: see [10]. The proof is based on the following Lyapunov function :

$$V = \frac{1}{2} \eta^T \eta \tag{73}$$

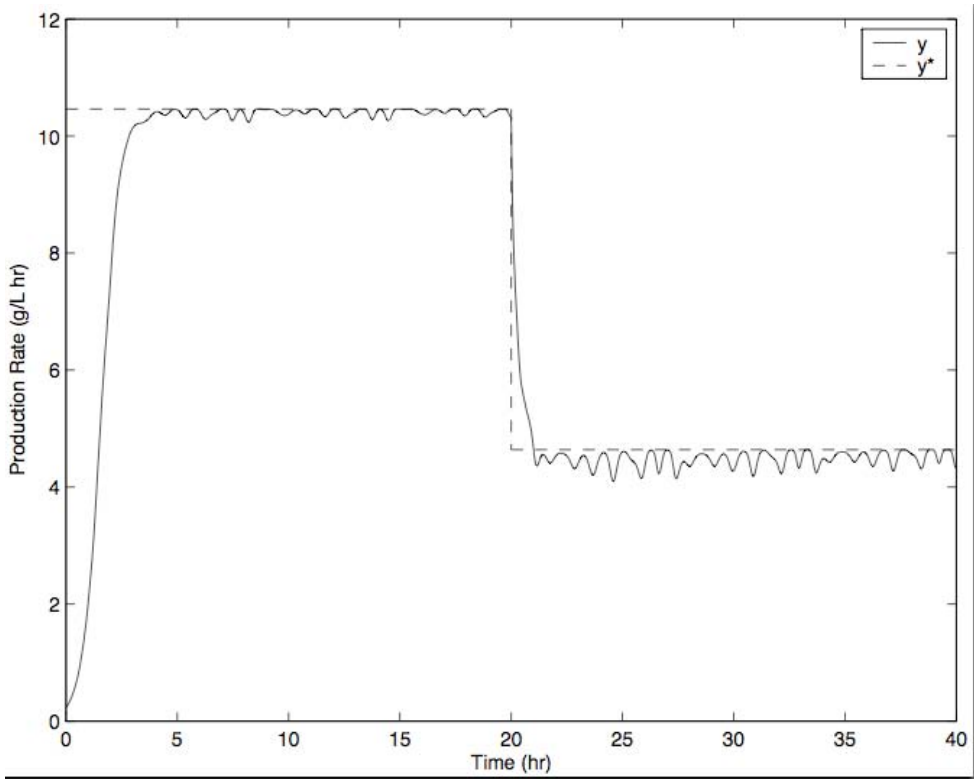

Figure 7: *Production rate y ("—") and its maximum y^* ("- -")*

Simulation results are shown in Figures 7 and **??**. We have considered here a bioreactor with the following growth kinetics :

$$\mu(s) = \frac{\mu_{m1} s}{K_{s1} + s + K_{I1} s^2} + \frac{\mu_{m2} s}{K_{s2} + s}$$

This model represents the growth of one biomass from one substrate via two parallel reaction pathways, one characterized by Haldane kinetics (and therefore possibly inhibited at high substrate concentration values) and the other characterized by Monod kinetics (with growth saturation at high substrate concentrations). The following parameter and initial values and design parameters' values have been considered :

$$\begin{aligned} K_{s1} &= 0.2, \mu_{m1} = 1.0, Y = 0.5, k_1 = 2.0, k_2 = 1.0, K_I 1 = 0.1, s_0 = 10.0 \\ K_{s2} &= 0.3, \mu_{m2} = 2.0, x(0) = 0.1, s(0) = 1, \hat{x}(0) = 0.1, \hat{s}(0) = 0.1 \\ \gamma_w &= 10.0, k_d = k_{z0} = k_{x0} = k_{s0} = k_4 = k_5 = k_6 = 1 \end{aligned}$$

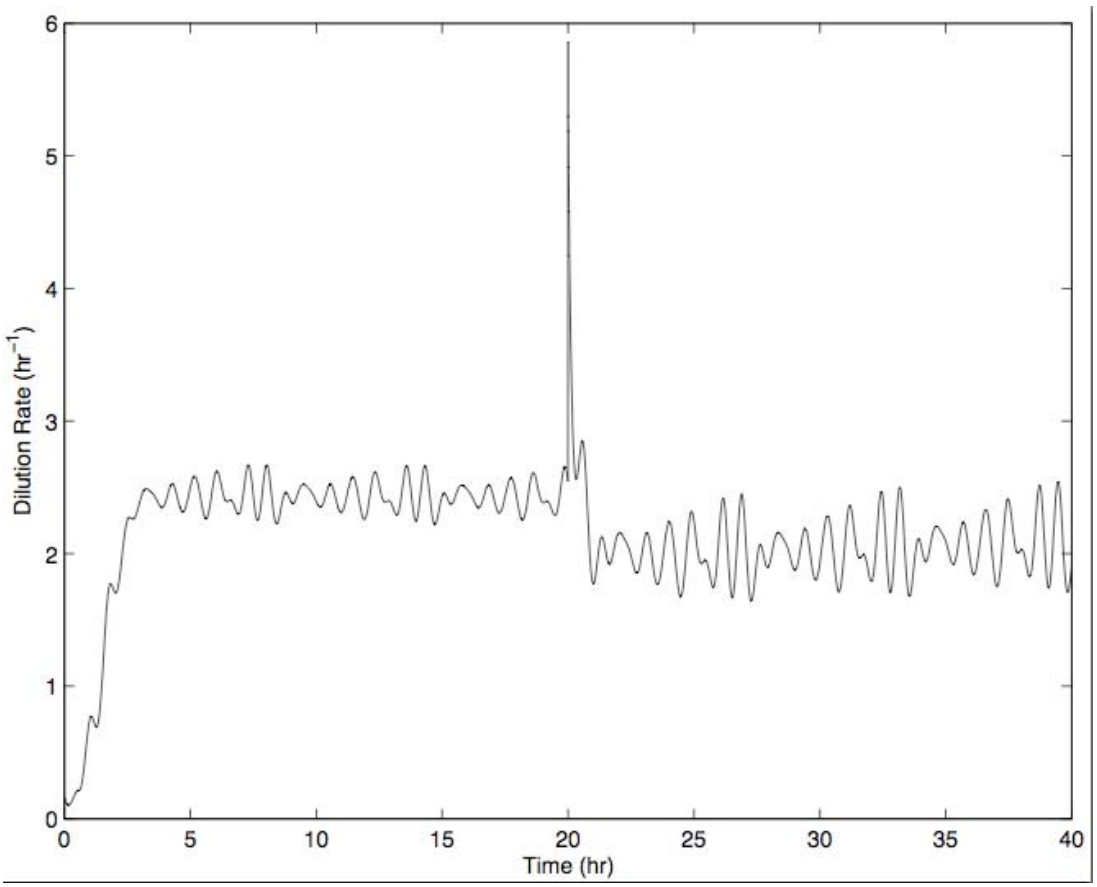

Figure 8: *Control input* $u(t)$

The NN radial basis function approximation consists of 5 terms with centers $\varphi_i = 1 + 10(i-1)/4$ and $\sigma_i = 1$ for $1 \leq i \leq 5$. The initial conditions for the adaptive learning weights are $\hat{W}_i(0) = 0.1, 1 \leq i \leq 5$. The dither signal was set to :

$$a(t) = \sum_{i=1}^{10} \omega_i \left(A_{1i} sin(\omega_i t) + A_{2i} cos(\omega_i t)\right)$$

where A_{1i} and A_{2i} are chosen as random numbers taken from a unit normal distribution. The frequencies are chosen as $\omega_i = 1 + (i-1)10/9$, $i = 1, \ldots, 10$, and $d(0) = \Upsilon(0) = 0$.

Acknowledgements. This paper presents research results of the Belgian Network DYSCO (Dynamical Systems, Control, and Optimization), funded by the Interuniversity Attraction Poles Programme, initiated by the Belgian State, Science Policy Office. The scientific responsibility rests with its authors.

4 Conclusions

The objective of this paper was to present a survey on extremum seeking control methods and their applications to process and reaction systems. Two important classes of extremum seeking control approaches have been considered : perturbation-based and model-based methods. For the latter, two options have been considered : with full model structure knowledge and with partial model structure knowledge. Theoretical stability and convergence results have been presented and simulations illutrate the performance of the approaches.

5 References

[1] Astrom K. J. and B. Wittenmark (1995). *Adaptive Control*, Addison-Wesley, 2nd edition, Reading, MA: Addison-Wesley.

[2] Bastin G. and D. Dochain (1990). *On-line Estimation and Adaptive Control of Bioreactors*, Elsevier, Amsterdam.

[3] Blackman P.F. (1962). Extremum-seeking regulators. In *An Exposition of Adaptive Control*, J.H. Westcott (ed.), The Macmillan Company, New York.

[4] Chioua M., B. Srinivasan, M. Guay and M. Perrier (2008). Dependence of the error in the optimal

solution of perturbation-based extremum-seeking methods on the excitation frequency. Submitted for publication.

[5] CougnonP., D. Dochain, M. Guay and M. Perrier (2006). Real-time optimization of a tubular reactor with distributed feed. *AIChE Journal*, 52(6), 2120–2128.

[6] Drkunov S., U. Ozguner, P. Dix and B. Ashrafi (1995). ABS control using optimum search via sliding modes. *IEEE Trans. Control Syst. Technol.*, 3, 79-85.

[7] Favache A., D. Dochain M. Perrier AND M. Guay (2008). Extremum seeking control of retention for a microparticulate system. To appear in *Can. J. Chem. Eng.*.

[8] Findeisen W., F.N. Bailey, M. Brdys, K. Malinowski, P. Tatjewski and A. Wozniak (1980). *Control and coordination in Hierarchical Systems,* John Wiley, New York.

[9] Guay M. and T. Zhang (2003). Adaptive Extremum Seeking Control of Nonlinear Dynamic Systems with Parametric Uncertainties. *Automatica*, 39(7), 1283-1293.

[10] Guay M., D. Dochain and M. Perrier (2004). Adaptive Extremum Seeking Control of Continuous Stirred Tank Bioreactors with Unknown Growth Kinetics. *Automatica*, 40, 881-888.

[11] Guay M., D. Dochain and M. Perrier (2005). Adaptive extremum seeking control of nonisothermal *CSTR*. *Chem. Eng. Science*, 60(13), 3671-3681.

[12] Guay M., D. Dochain, M. Perrier and N. Hudon (2007). Flatness-Based Extremum Seeking Control Over Periodic Orbits. IEEE Trans. Aut. Control, 52 (10), 2005-2012.

[13] Hudon N., M. Perrier, M. Guay and D. Dochain (2004). Adaptive Extremum Seeking Control of a Non-Isothermal Tubular Reactor With Unknown Kinetics. *Comp. Chem. Eng.*, 29 (4), 839-849.

[14] Hudon N., M. Guay, M. Perrier and D. Dochain (2008). Adaptive Extremum-Seeking Control of Convection-Reaction Distributed Reactor with Limited Actuation. To appear in *Comp. Chem. Eng.*.

[15] Ioannou P. A. and J. Sun (1996). *Robust Adaptive Control,* Englewood Cliffs, NJ: Prentice-Hall.

[16] Khalil H.K. (2002). *Nonlinear Systems*. Prentice-Hall, Upper Saddle River, NJ.

[17] Krstic M., I. Kanellakopoulos, and P. Kokotovic (1995). *Nonlinear and Adaptive Control Design,* New York: Wiley and Sons.

[18] Krstic M. (2000). Performance Improvement and Limitation in Extremum Seeking Control. *Systems & Control Letters*, 39 (5), 313-326.

[19] Krstic M. and H.H. Wang (2000). Stability of Extremum Seeking Feedback for General Dynamic Systems. *Automatica*, 36 (4), 595-601.

[20] Landau Y. D. (1979) *Adaptive Control*, New York: Marcel Dekker.

[21] Leblanc M. (1922). Sur l'életrification des chemins de fer au moyen de courants alternatifs de fréquence élevée. *Revue Générale de l'Electricité*.

[22] Marcos N., M. Guay, D. Dochain and T. Zhang (2003). Adaptive extremum seeking control of a continuous bioreactor. *J. Proc. Control*, 14 (3), 317-328.

[23] Marcos N., M. Guay and D. Dochain (2004). Output feedback adaptive extremum seeking control of a continuous stirred tank bioreactor with MonodÕs kinetics. *J. Proc. Control*, Special issue on Dynamics, Monitoring, Control and Optimization of Biological Systems, 14(7), 807-818.

[24] Marlin T.E. and A.N. Hrymak (1997). Real-time operations optimization of continuous processes. In *5th Int. Conf. Chemical Process Control*, J.C. Kantor, C. Garcia & B. Carnahan (Eds.), AIChE Symp. Series 316, Vol. 93, 156-164.

[25] Morari M. , G. Stephanopoulos and Y. Arkun (1980). Studies in the synthesis of control structures for chemical processes. Part I: Formulation of the problem. Process decomposition and the classification of the control task. Analysis of the optimizing control structures. *AIChE J.*, 26(2), 220-232.

[26] Sanner R.M. and J.J. E. Slotine (1992). Gaussian networks for direct adaptive control. *EEE Trans. Neural Networks*, 3(6), 837-863.

[27] Seshagiri S. and H.K. Khalil (2000). Output feedback control of nonlinear systems using RBF neural networks. *IEEE Trans. Neural Networks*, 11(1),69-79.

[28] Sternby J. (1980). Extremum control systems: An area for adaptive control?" Preprints of the *Joint American Control Conference,* San Fancisco, CA, WA2-A.

[29] Skogestad S. (2000). Plantwide control: the search for the self-optimizing control structure. *J. Proc. Control*, 10, 487-507.

[30] Titica M., D. Dochain and M. Guay (2003). Adaptive extremum seeking control of fedbatch bioreactors. *Eur. J. Control*, 9(6), 618-631.

[31] Titica M., D. Dochain and M. Guay (2003). Real-time Optimisation of fedbatch bioreactors via adaptive extremum seeking control. *Chem. Eng. Res. Des.*, 81 (A9): 1289-1295.

[32] Vasu G. (1957). Experiments with optimizing controls applied to rapid control of engine presses with high amplitude noise signals. *Trans. ASME,* 481-488.

[33] Wang H.H., S. Yeung and M. Krstic (1998). Experimental Application of Extremum Seeking on an Axial Flow Compressor. *Proc. ACC*,1989-1993.

[34] Wang H.H., M. Krstic and G. Bastin (1999). Optimizing bioreactors by extremum seeking. *Int. J. Adaptive Control & Signal Processing*, 13(8),651-669.

[35] Wittenmark B. and J. Evans (2001). Extremal control of Wiener model processes. *Dept Aut. Control,*

Lund Inst. Technol., Int. rep., ISRN LUTFD2 TFRT7599SE.

[36] Yaodong P., U. Ozguner U and T. Acarman (2003). Stability and performance improvement of extremum seeking control with sliding mode. *Int. J. Control*, 76(9-10), 968–985.

[37] Zhang Y., D. Monder and J.F. Forbes (2002). Real-time optimization under parametric uncertainty: A probability constrained approach. *J. Proc. Control*,12(3), 373-389.

[38] Zhang T., M. Guay and D. Dochain (2003). Adaptive extremum seeking control of continuous stirred tank bioreactors. *AIChE J.*, 49 (1), 113-123.